

Light Sterile Neutrinos: Models and Phenomenology

James Barry,^{*} Werner Rodejohann,[†] and He Zhang[‡]

*Max-Planck-Institut für Kernphysik,
Postfach 103980, 69029 Heidelberg, Germany*

Abstract

Motivated by recent hints in particle physics and cosmology, we study the realization of eV-scale sterile neutrinos within both the seesaw mechanism and flavor symmetry theories. We show that light sterile neutrinos can rather easily be accommodated in the popular A_4 flavor symmetry models. The exact tri-bimaximal mixing pattern is perturbed due to active-sterile mixing, which we discuss in detail for one example. In addition, we find an interesting extension of the type I seesaw, which can provide a natural origin for eV-scale sterile neutrinos as well as visible admixtures between sterile and active neutrinos. We also show that the presence of sterile neutrinos would significantly change the observables in neutrino experiments, specifically the oscillation probabilities in short-baseline experiments and the effective mass in neutrino-less double beta decay. The latter can prove particularly helpful in strengthening the case for eV-scale sterile neutrinos.

^{*}Electronic address: james.barry@mpi-hd.mpg.de

[†]Electronic address: werner.rodejohann@mpi-hd.mpg.de

[‡]Electronic address: he.zhang@mpi-hd.mpg.de

I. INTRODUCTION

Neutrino oscillation experiments have provided firm evidence that, in contrast to the prediction of the Standard Model (SM), neutrinos are massive and that their flavors change during propagation. Their unusual mixing pattern and the smallness of their masses makes the explanation of the origin of neutrino masses and leptonic flavor mixing one of the most challenging problems in particle physics. In the standard neutrino oscillation picture three active neutrinos are involved, with mass-squared differences of order 10^{-4} and 10^{-3} eV². The absolute mass scale of neutrinos is also constrained to be less than around 1 eV from tritium beta decay experiments as well as cosmological observations. For a recent review on our current understanding of neutrino observables, see Ref. [1].

Despite the successful achievements of solar, atmospheric, reactor and accelerator neutrino experiments, there are experimental anomalies that cannot be explained within the standard three neutrino framework. In particular, the possible presence of sterile neutrinos points towards non-standard neutrino physics. The issue of the LSND and MiniBooNE results has been around for some time, and is frequently interpreted as a hint towards the presence of one or two sterile neutrino states [2–5]. Recently this debate has been re-ignited by a reevaluation of the anti-neutrino spectra of nuclear reactors [6], which leads to increased fluxes. As a result, the negative results of previous reactor experiments can in fact be interpreted as the observation of a flux deficit, and this in turn can be explained by additional sterile neutrinos with masses at the eV scale [6, 7]. Interestingly, current results from precision cosmology and Big Bang nucleosynthesis mildly favor extra radiation in the Universe beyond photons and ordinary neutrinos. While this could be any relativistic degree of freedom, the interpretation in terms of additional sterile neutrino species is straightforward. Indeed, several cosmological parameter fits (e.g., the analyses of the CMB or SDSS data sets in Ref. [8]) have been found to be compatible with more radiation than that predicted by the SM particle content. This is supported by the recently reported higher ⁴He abundance [9, 10], which in the framework of Big Bang nucleosynthesis can be accommodated by additional relativistic degrees of freedom, as it leads to earlier freeze-out of the weak reactions, resulting in a higher neutron-to-proton ratio. It is rather intriguing that hints for the presence of sterile neutrinos are given by fundamentally different probes: neutrino oscillations, Big Bang nucleosynthesis and observation of the Universe’s structure. This is the situation which motivates the present study.

Sterile neutrinos, if they exist, would lead to rich experimental phenomena. By definition, sterile neutrinos do not directly enter the weak interactions. However, their admixture with active neutrinos would modify the neutrino flavor mixing and lead to observable effects in neutrino oscillation experiments. Furthermore, due to that admixture they could interact with gauge bosons, resulting in significant corrections to certain non-oscillation processes, e.g., in the neutrino-less double decay ($0\nu\beta\beta$) amplitude [11–13] or in beta decay spectra, such as in the KATRIN experiment [14, 15]. It has also been pointed out that an eV-scale

sterile neutrino would significantly affect the the atmospheric neutrino fluxes in the energy range 500 GeV to a few TeV, and these effects could be studied in the IceCube detector [16–18]. Other aspects that are in principle modified by such sterile states are supernova physics [19], solar neutrinos [20], or the interpretation of cosmological data [21]. We will add to this discussion by updating the predictions for $0\nu\beta\beta$ with the recent results for the relevant mixing parameters. We consider all possible neutrino mass spectra, namely four in case of one sterile neutrino, and eight in case of two sterile neutrinos. For the latter case we also point out some properties of short-baseline oscillation probabilities in four often overlooked possible spectra.

On the other hand, we consider the non-trivial theoretical origin of eV-scale sterile neutrinos. In what regards neutrino masses and their peculiar mixing structure, the key words are seesaw mechanism [22–25] and flavor symmetries (see [26, 27] for recent reviews). We will show that popular models based on the A_4 flavor symmetry can easily be modified to take sterile neutrinos into account. As a result, the mixing structure of the original model, tri-bimaximal mixing (TBM) in our example, is perturbed, and corrections to the tri-bimaximal values arise. This will be a general feature of such approaches, but here we focus on one concrete example, which we will outline in detail.¹

Sterile neutrinos are a necessary ingredient of the canonical type I seesaw mechanism, though they are naturally assumed to be many orders of magnitude heavier than the SM scale of 10^2 GeV. As a result, their mixing with the SM particles is highly suppressed. If one brings one of the heavy states down to the eV scale, it is possible to generate a sterile neutrino with the correct mass and (potentially) the correct mixing with the SM leptons to explain the data. However, another more non-trivial case can also be studied, namely an extension of the type I seesaw with additional heavy (i.e. heavier than the SM scale) neutral fermions. This approach generates sterile neutrinos without the need to initially have states with eV masses, and is more in the seesaw spirit.

The remaining parts of this work are organized as follows: in Sec. II, we outline the formalism of neutrino mixing in the presence of sterile states and summarize the phenomenological consequences of sterile neutrinos in neutrino-less double beta decay. Short comments on short-baseline neutrino oscillations are delegated to the Appendix. Then, in Sec. III, we discuss how to embed sterile neutrinos into one particular A_4 flavor symmetry model, and describe the resulting deviations from exact TBM. Section IV is devoted to a general overview of the realization of sterile neutrinos in seesaw models. Finally, we conclude in Sec. V. The individual sections are largely independent of each other, but their results and methods could be combined. However, we feel that a separate discussion of each aspect is more suitable for the present discourse.

¹ Note that a general analysis of the mixing of active and sterile neutrinos has been presented in Ref. [28].

II. PHENOMENOLOGICAL CONSEQUENCES OF STERILE NEUTRINOS

In this section we will outline some properties of neutrino parameters and evaluate the contributions to the effective mass relevant for neutrino-less double beta decay.

A. Neutrino mixing with sterile neutrinos

In the presence of $n_s = n - 3$ sterile neutrinos, the neutrino mass matrix is an $n \times n$ matrix m_ν , which can be diagonalized by means of an $n \times n$ unitary matrix U . The neutrino flavor eigenstates ν_f (for $f = e, \mu, \tau, s_1, s_2, \dots, s_{n-3}$) are then related to their mass eigenstates ν_i (for $i = 1, 2, \dots, n$) via

$$\nu_f = \sum_{i=1}^n U_{fi} \nu_i. \quad (1)$$

In general, for n massive families including $n_s = n - 3 \neq 0$ massive sterile neutrinos, one has $n - 1 = n_s + 2$ Majorana phases, $3(n - 2) = 3(n_s + 1)$ mixing angles and $2n - 5 = 2n_s + 1$ Dirac phases. The number of angles and Dirac phases is less than the naive $\frac{1}{2}n(n - 1)$ angles and $\frac{1}{2}(n - 1)(n - 2)$ phases, because the $\frac{1}{2}n_s(n_s - 1)$ rotations between sterile states are unphysical. For illustration, in the case of only one sterile neutrino, U is typically parameterized by

$$U = R_{34} \tilde{R}_{24} \tilde{R}_{14} R_{23} \tilde{R}_{13} R_{12} P, \quad (2)$$

where the matrices R_{ij} are rotations in ij space, i.e.

$$R_{34} = \begin{pmatrix} 1 & 0 & 0 & 0 \\ 0 & 1 & 0 & 0 \\ 0 & 0 & c_{34} & s_{34} \\ 0 & 0 & -s_{34} & c_{34} \end{pmatrix} \quad \text{or} \quad \tilde{R}_{14} = \begin{pmatrix} c_{14} & 0 & 0 & s_{14}e^{-i\delta_{14}} \\ 0 & 1 & 0 & 0 \\ 0 & 0 & 1 & 0 \\ -s_{14}e^{i\delta_{14}} & 0 & 0 & c_{14} \end{pmatrix}, \quad (3)$$

where $s_{ij} = \sin \theta_{ij}$, $c_{ij} = \cos \theta_{ij}$. The diagonal P matrix contains the three Majorana phases α , β and γ :

$$P = \text{diag} \left(1, e^{i\alpha/2}, e^{i(\beta/2+\delta_{13})}, e^{i(\gamma/2+\delta_{14})} \right). \quad (4)$$

Note that there are in total three Dirac CP-violating phases δ_{ij} . The above definition of P is constructed in such a way that only Majorana phases show up in the effective mass governing neutrino-less double beta decay (see below). Similarly, one can parameterize the mixing matrix for 2 sterile neutrinos as

$$U = \tilde{R}_{25} R_{34} R_{25} \tilde{R}_{24} R_{23} \tilde{R}_{15} \tilde{R}_{14} \tilde{R}_{13} R_{12} P, \quad (5)$$

where $P = \text{diag}(1, e^{i\alpha/2}, e^{i(\beta/2+\delta_{13})}, e^{i(\gamma/2+\delta_{14})}, e^{i(\phi/2+\delta_{15})})$.

The mass-squared differences associated with the current hints for sterile neutrinos are much larger than the ones responsible for solar and atmospheric oscillations. The sterile neutrinos are thus separated in mass from the active ones and can either be heavier or lighter than the active ones. The active neutrinos can be normally ($m_3 > m_2 > m_1$) or inversely ($m_2 > m_1 > m_3$) ordered. Therefore, if there is one sterile neutrino, there are in total four possible mass orderings. Our nomenclature for the schemes is such that we go from top to bottom, i.e. if $m_s \gg m_{1,2,3}$, we denote this 1+3 scenario as “SN” if the active neutrinos are normally ordered and “SI” if they are inversely ordered. Analogously, if the sterile state is lighter than the active ones ($m_{1,2,3} \gg m_s$, 3+1 scenario), we name the schemes “NS” and “IS”, respectively. Obviously, 3+1 scenarios are less attractive since they induce (more) tension with the cosmological bound on the sum of neutrino masses. The models we will present in later sections indeed predict 1+3 scenarios.

In the case of two sterile neutrinos with masses m_{s_1} and m_{s_2} , there are three classes of mass spectra: $m_{s_1}, m_{s_2} \gg m_{1,2,3}$ (2+3 scenarios), $m_{1,2,3} \gg m_{s_1}, m_{s_2}$ (3+2) and [13] $m_{s_2} \gg m_{1,2,3} \gg m_{s_1}$ (1+3+1). The latter class of 1+3+1 orderings, first noted in Ref. [13], has received less attention in the past, and was for instance not taken into account in the fits of Refs. [2–4]. The 1+3+1 cases have the interesting property that the active states are sandwiched between the two sterile ones. Current oscillation data cannot distinguish 1+3 from 3+1, or 3+2 from 2+3 scenarios, but are sensitive to 1+3+1 vs. 2+3/3+2 (see the Appendix). Ref. [7] fits the world’s short-baseline data also within the 1+3+1 scenario and finds that the fit is slightly better than that for 2+3/3+2. The 2+3 cases are denoted “SSN” or “SSI”, while the 3+2 cases are called “NSS” or “ISS”. In what regards the 1+3+1 cases, two possible permutations of the mass spectrum should be distinguished. One of the sterile neutrinos is separated from the active ones by a larger mass gap, associated with the larger of the two mass-squared differences. If the heavier of the two sterile neutrinos is connected with the larger mass-squared difference, the scenarios are denoted “SNSa” and “SISa”, respectively; if the heavier sterile state is connected with the smaller mass-squared difference, we call the cases “SNSb” and “SISb”. The 2+3 scenarios are more attractive than the others because they predict a smaller sum of masses. The individual masses $m_{1,2,3,4,5}$ expressed in terms of the mass-squared differences Δm_S^2 , Δm_A^2 , Δm_{41}^2 and Δm_{51}^2 can be found in Ref. [13], where the generalization to three sterile neutrinos (with sixteen possible mass orderings) is also discussed.

Table I shows the best-fit and 2σ ranges of the relevant parameters used for the analysis in this work. The best-fit values are taken from the global fit in Table II of Ref. [7]. In their analysis of the 3+1/1+3 scenarios, the authors of Ref. [7] find several different allowed regions in the $\Delta m_{41}^2 - \sin^2\theta_{14}$ parameter space, at 2σ . For convenience we use the region around the best-fit point, and (since the ranges are not available) allow the parameters in

TABLE I: Best-fit (from Ref. [7]) and estimated 2σ values of the sterile neutrino parameters.

	parameter	Δm_{41}^2 [eV]	$ U_{e4} ^2$	Δm_{51}^2 [eV]	$ U_{e5} ^2$
3+1/1+3	best-fit	1.78	0.023		
	2σ	1.61–2.01	0.006–0.040		
3+2/2+3	best-fit	0.47	0.016	0.87	0.019
	2σ	0.42–0.52	0.004–0.029	0.77–0.97	0.005–0.033
1+3+1	best-fit	0.47	0.017	0.87	0.020
	2σ	0.42–0.52	0.004–0.029	0.77–0.97	0.005–0.035

the 3+2, 2+3 and 1+3+1 cases to have 2σ uncertainties of the same relative magnitude as those in the 3+1/1+3 scenario. The data favor the presence of two sterile neutrinos, mostly because they allow different neutrino and anti-neutrino probabilities, thus alleviating the tension between the LSND and MiniBooNE results. As mentioned above, 1+3+1 scenarios have a slightly better fit than 3+2/2+3 cases.

We note in addition that the recent results from the T2K [29] and MINOS [30] experiments strengthen the existing hints [31–33] for non-zero θ_{13} , and that the analysis in Ref. [34] finds evidence for $\theta_{13} > 0$ at the level of $> 3\sigma$. It is not yet evident whether these new data will improve or worsen the fits in the various sterile neutrino scenarios; on the other hand it can also be argued that the T2K result is not due to θ_{13} but is actually another signature of sterile neutrinos [35].

B. Neutrino-less double beta decay

Neutrino-less double beta decay ($0\nu\beta\beta$) is the only realistic test of lepton number violation. While there are several mechanisms to mediate the process (e.g. heavy neutrinos, right-handed currents or SUSY particles), light Majorana neutrino exchange is presumably the best motivated scenario. We will work in this standard interpretation of $0\nu\beta\beta$, and study the effect of massive sterile neutrinos in the eV range. This section is an update of the results in Refs. [12, 13]; we also use the best-fit values in Table I to report approximate numerical lower limits for the complementary mass observables $m_\beta \equiv \sqrt{|U_{ei}|^2 m_i^2}$ and $\sum m_i$, constrained by beta decay and cosmology, respectively.

In the presence of one sterile neutrino, the effective neutrino mass in $0\nu\beta\beta$ is given by

$$\langle m_{ee} \rangle_{4\nu} = \left| c_{12}^2 c_{13}^2 c_{14}^2 m_1 + s_{12}^2 c_{13}^2 c_{14}^2 m_2 e^{i\alpha} + s_{13}^2 c_{14}^2 m_3 e^{i\beta} + s_{14}^2 m_4 e^{i\gamma} \right|, \quad (6)$$

using the parameterization in Eq. (2). If the sterile neutrino is heavier than the active ones, the approximation

$$\langle m_{ee} \rangle_{(1+3)\nu} \simeq \left| c_{14}^2 \langle m_{ee} \rangle_{3\nu} + s_{14}^2 \sqrt{\Delta m_{41}^2} e^{i\gamma} \right| \quad (7)$$

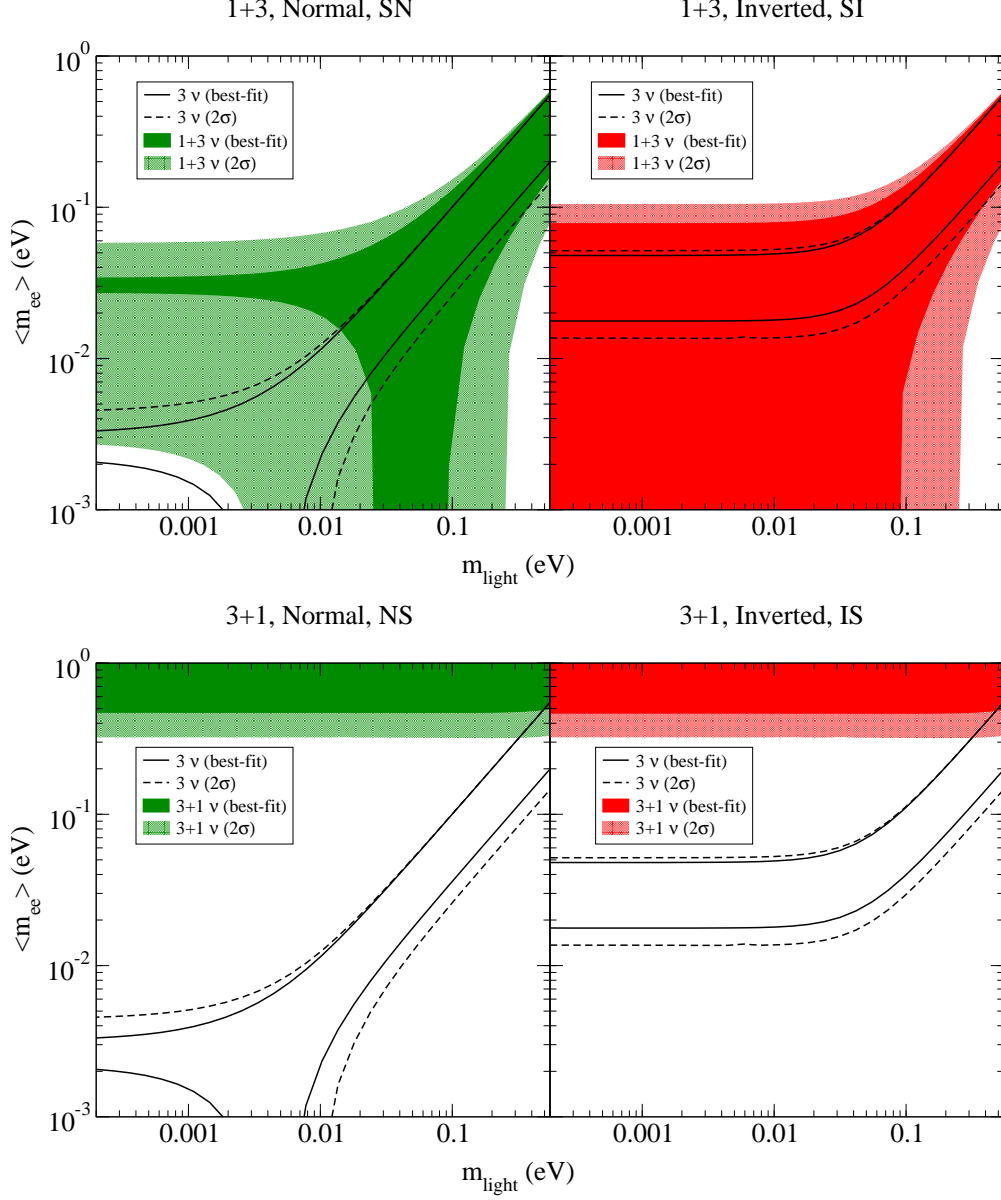


FIG. 1: The allowed ranges in the $\langle m_{ee} \rangle - m_{\text{light}}$ parameter space, both in the standard three-neutrino picture (unshaded regions) and with one sterile neutrino (shaded regions), for the 1+3 (top) and 3+1 (bottom) cases.

holds, where $\langle m_{ee} \rangle_{3\nu} = c_{12}^2 c_{13}^2 m_1 + s_{12}^2 c_{13}^2 m_2 e^{i\alpha} + s_{13}^2 m_3 e^{i\beta}$ is the standard expression for three active neutrinos. The upper panel of Fig. 1 displays the allowed range of $\langle m_{ee} \rangle_{(1+3)\nu}$ as a function of the lightest mass m_{light} , using data from Refs. [7, 33]. Also shown in this plot and the following ones is the allowed range of $|\langle m_{ee} \rangle_{3\nu}|$, i.e. the standard case. Its crucial features (see [36] and references therein) are that $|\langle m_{ee} \rangle_{3\nu}|$ can vanish exactly in the normal hierarchy case, but cannot vanish in neither the inverted hierarchy nor the quasi-degenerate case. This standard behavior can be completely mixed up by the presence of one or more sterile neutrinos: if the lightest neutrino mass is reasonably small, e.g. $m_{\text{light}} < 0.01$ eV, the

allowed range of $\langle m_{ee} \rangle_{(1+3)\nu}$ is dominated by the term $s_{14}^2 \sqrt{\Delta m_{41}^2} \simeq 0.031$ eV, which means that $\langle m_{ee} \rangle_{(1+3)\nu}$ cannot vanish in the normal ordering case (the contribution of the two light active neutrinos cannot cancel that of the sterile neutrino). However, in the inverted ordering $\langle m_{ee} \rangle_{(1+3)\nu}$ can vanish even for very small active neutrino masses. The effective mass can also be zero in the regime where the active neutrinos are quasi-degenerate ($m_{\text{light}} > 0.1$ eV).

This modified behavior of $\langle m_{ee} \rangle$ is of particular interest in the inverted ordering case, since the usual lower bound on the effective mass (cf. the solid and dashed lines in Fig. 1) is no longer valid. If future $0\nu\beta\beta$ experiments measure a tiny effective mass and the neutrino mass hierarchy is confirmed to be inverted from long-baseline neutrino oscillations, the sterile neutrino hypothesis would be an attractive explanation for this inconsistency. In the 3+1 case, m_β and $\sum m_i$ are dominated by the sterile contribution, i.e. $m_\beta \gtrsim \sqrt{|U_{e4}|^2 \Delta m_{41}^2} \simeq 0.2$ eV and $\sum m_i \gtrsim \sqrt{\Delta m_{41}^2} \simeq 1.3$ eV, respectively.

The lower panel of Fig. 1 shows the effective mass when the sterile neutrino is lighter than the active ones (the 3+1 scenario). In this case there are three quasi-degenerate neutrinos at the eV scale, with their mass given by $\sqrt{\Delta m_{41}^2} \simeq 1.3$ eV (this mass scale governs predictions for m_β). The effective mass then takes its standard form for quasi-degenerate neutrinos:

$$\langle m_{ee} \rangle_{(3+1)\nu} \simeq \sqrt{\Delta m_{41}^2} \sqrt{1 - \sin^2 2\theta_{12} \sin^2 \alpha/2}. \quad (8)$$

However, this situation is relatively disfavored by cosmological bounds on the sum of neutrino masses [8], since $\sum m_i \gtrsim 3\sqrt{\Delta m_{41}^2} \simeq 4$ eV. If taken at face value, the current limit of about 0.5 eV on the effective mass means that $\sqrt{1 - \sin^2 2\theta_{12} \sin^2 \alpha/2} \lesssim 0.4$, thus already putting strong constraints on the solar neutrino mixing angle and in particular the Majorana phase.

If there are two sterile neutrinos, the effective mass reads

$$\langle m_{ee} \rangle_{5\nu} = \left| c_{12}^2 c_{13}^2 c_{14}^2 c_{15}^2 m_1 + s_{12}^2 c_{13}^2 c_{14}^2 c_{15}^2 m_2 e^{i\alpha} + s_{13}^2 c_{14}^2 c_{15}^2 m_3 e^{i\beta} + s_{14}^2 c_{15}^2 m_4 e^{i\gamma} + s_{15}^2 m_5 e^{i\phi} \right|, \quad (9)$$

with ϕ the additional Majorana phase. In the 2+3 cases where both of the sterile neutrinos are at the eV scale, $\langle m_{ee} \rangle$ can be approximated by

$$\langle m_{ee} \rangle_{(2+3)\nu} \simeq \left| c_{14}^2 c_{15}^2 \langle m_{ee} \rangle_{3\nu} + s_{14}^2 \sqrt{\Delta m_{41}^2} e^{i\gamma} + s_{15}^2 \sqrt{\Delta m_{51}^2} e^{i\phi} \right|, \quad (10)$$

in analogy to the 1+3 case. The upper panel of Fig. 2 shows the allowed regions in this case: the phenomenology is similar to that discussed for 1+3 above, except that the presence of two sterile terms in Eq. (10) allows $\langle m_{ee} \rangle$ to take smaller values in the hierarchical region for the normal ordering. The inverted ordering is essentially the same as in the 1+3 case. The two eV-scale sterile neutrinos dominate the KATRIN observable, with

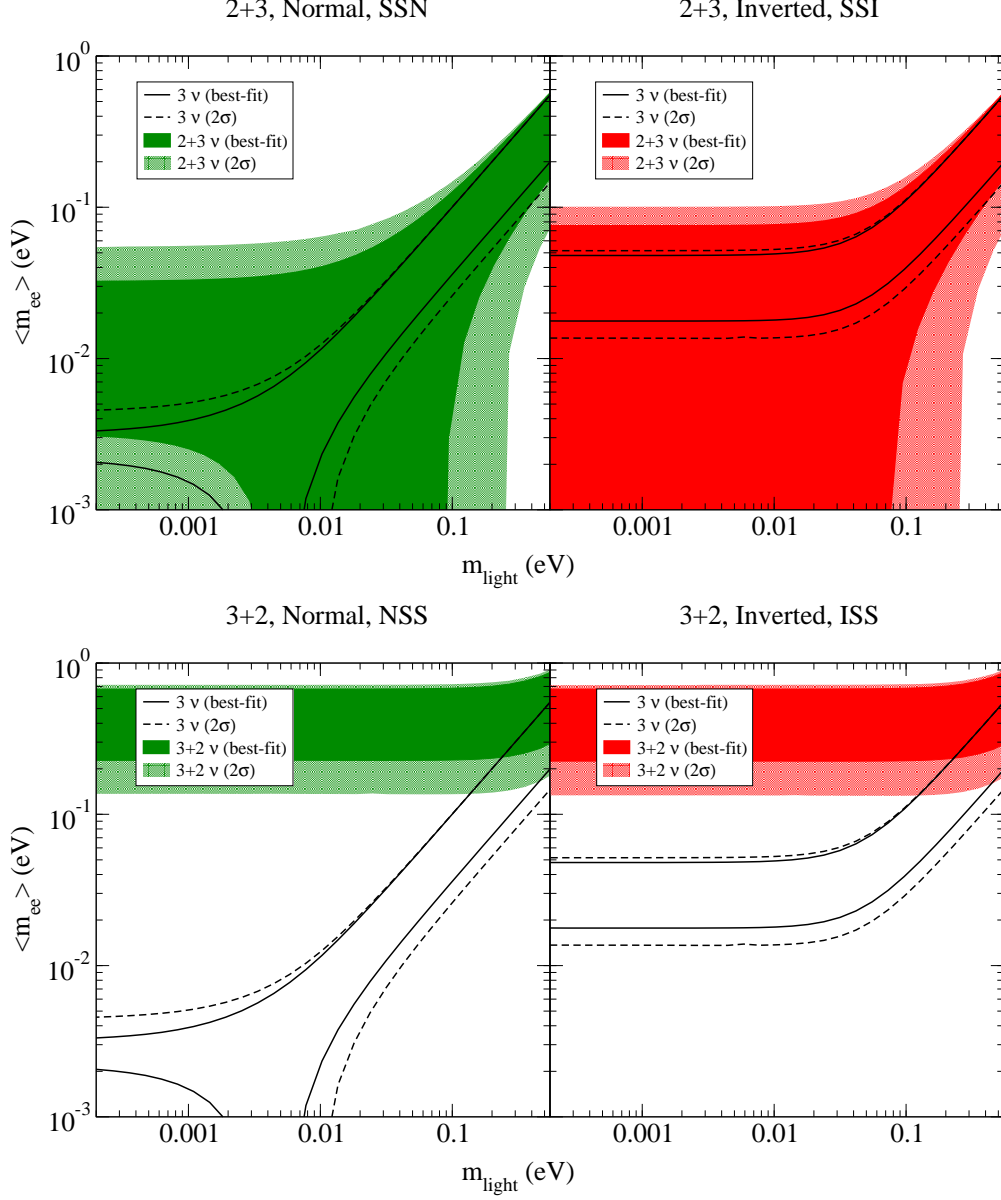


FIG. 2: Same as Fig. 1, for the 2+3 (top) and 3+2 (bottom) cases.

$m_\beta \gtrsim \sqrt{|U_{e4}|^2 \Delta m_{41}^2 + |U_{e5}|^2 \Delta m_{51}^2} \simeq 0.16$ eV, and the sum of masses is approximately $\sum m_i \gtrsim \sqrt{\Delta m_{41}^2} + \sqrt{\Delta m_{51}^2} \simeq 1.6$ eV.

The lower panel of Fig. 2 displays the 3+2 cases, where the sterile neutrinos are lighter than the active ones. Since the three active neutrinos are quasi-degenerate at the eV scale, with their mass given by the largest sterile mass-squared difference $\sqrt{\Delta m_{41}^2} \simeq 0.69$ eV, Eq. (8) applies for $\langle m_{ee} \rangle_{(3+2)\nu}$ and the value of m_β is also set by this scale. The mass ordering of the active states plays no role. Once again these scenarios are disfavored by cosmology, since $\sum m_i \gtrsim 3\sqrt{\Delta m_{51}^2} + \sqrt{\Delta m_{51}^2 - \Delta m_{41}^2} \simeq 3.4$ eV.

For completeness we include plots of the effective mass in the 1+3+1 schemes, where the active neutrinos are sandwiched between the sterile ones. The plots in Fig. 3 show

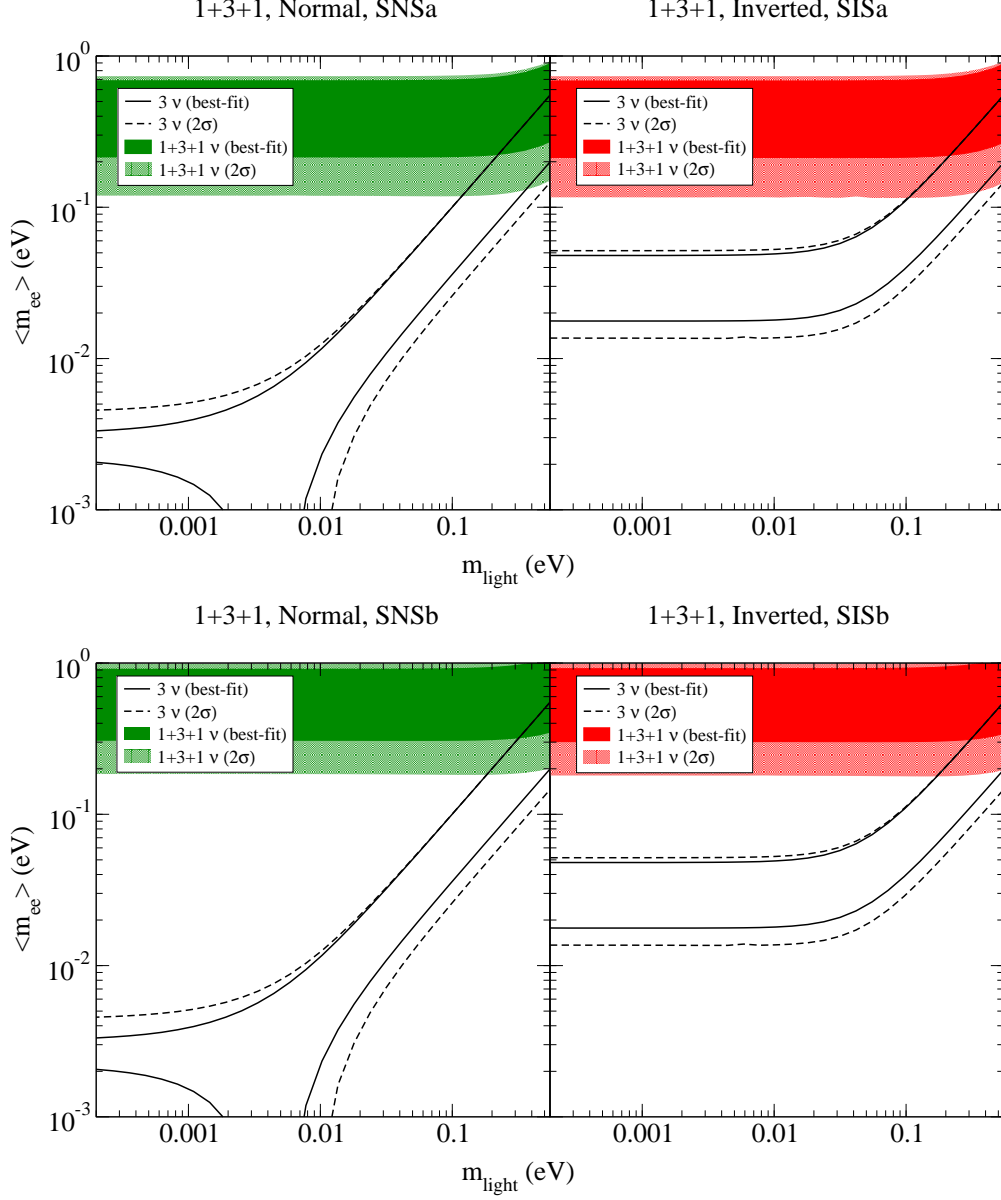


FIG. 3: Same as Fig. 1, for the 1+3+1a (top) and 1+3+1b (bottom) cases.

that there is little difference between these scenarios and the 3+2 cases. The main difference arises in SNSb and SISb scenarios, in which the effective mass is governed by three quasi-degenerate neutrinos with mass $\sqrt{\Delta m_{51}^2} \simeq 0.93$ eV, plus a (coherent) contribution of $|U_{e4}|^2 \sqrt{\Delta m_{41}^2 + \Delta m_{51}^2} \simeq 0.03$ eV. The KATRIN observable is also dominated by this mass scale, and the sum of masses is $\sum m_i \gtrsim 3\sqrt{\Delta m_{51}^2} + \sqrt{\Delta m_{41}^2 + \Delta m_{51}^2} \simeq 4.0$ eV.

The results of this section will not be significantly modified in the presence of new data [29] on $\sin^2\theta_{13}$. In the hierarchical region with normal ordering, the lower limit on the effective mass decreases with $\sin^2\theta_{13}$, so that the larger best-fit value from Ref. [34] would have a small effect on $\langle m_{ee} \rangle$ in the standard three-neutrino scenario. However, in the sterile case the dominant terms in Eqs. (7) and (10) are independent of $\sin^2\theta_{13}$.

As discussed in the different cases above, if the predictions of the effective mass are above 0.2 eV, which is true for most of the possible scenarios, then KATRIN will see a signal as well. Indeed, Refs. [14, 15] show that sterile neutrinos with masses and mixings in the ranges considered above will be observable in KATRIN, and will be distinguishable from active neutrinos. This effect should be seen in almost all cases; the smallest contribution to the observable m_β arises in the SSN and SSI cases.

In what regards the sum of masses, the smallest result holds again for SSN and SSI ($\sum m_i \gtrsim 1.6$ eV); the value of $\sum m_i$ exceeds this in all other cases. The current upper bound from cosmology is approximately $\sum m_i \lesssim 0.5$ eV [37], which introduces tension with the sterile neutrino scenarios presented above. However, this measurement is highly model dependent and depends on the cosmological data set used. The Planck satellite should in the near future be able to reach a sensitivity of ~ 0.1 eV, thus providing more precise limits on the absolute neutrino mass. In addition, the present hints for extra radiation from analysis of CMB anisotropy measurements will be further constrained by Planck data, with a precision of $\Delta N_{\text{eff}} \sim \pm 0.3$ [8, 38], where N_{eff} is the effective number of thermally excited neutrino degrees of freedom. This means that Planck could in fact rule out a sterile neutrino species before beta decay or $0\nu\beta\beta$ experiments see a signal.

III. STERILE NEUTRINOS IN FLAVOR SYMMETRY MODELS: AN A_4 EXAMPLE

In this section we modify a popular flavor symmetry model, which predicts tri-bimaximal mixing and is based on the group A_4 , in order to accommodate one or two light sterile neutrinos.

A. One sterile neutrino

In the Altarelli-Feruglio A_4 model from Ref. [39], neutrinos get mass from effective operators, and the judicious choice of particle and flavon content along with the correct vacuum expectation value (VEV) alignment leads to TBM. The relevant particle assignments are shown in Table II. Note the presence of an additional Z_3 symmetry to separate the neutrino and charged lepton sectors, and the Froggatt-Nielsen $U(1)_{\text{FN}}$ to generate a hierarchy for the charged lepton masses. We have also included a sterile neutrino ν_s with appropriate quantum numbers under the symmetries.

Leaving ν_s aside for the moment, these particle assignments, along with the A_4 multipli-

TABLE II: Particle assignments of the A_4 model, modified from Ref. [39] to include a sterile neutrino ν_s . The additional Z_3 symmetry decouples the charged lepton and neutrino sectors; the $U(1)_{\text{FN}}$ charge generates the hierarchy of charged lepton masses and regulates the scale of the sterile state.

Field	L	e^c	μ^c	τ^c	$h_{u,d}$	φ	φ'	ξ	ν_s
$SU(2)_L$	2	1	1	1	2	1	1	1	1
A_4	$\underline{3}$	$\underline{1}$	$\underline{1}''$	$\underline{1}'$	$\underline{1}$	$\underline{3}$	$\underline{3}$	$\underline{1}$	$\underline{1}$
Z_3	ω	ω^2	ω^2	ω^2	1	1	ω	ω	1
$U(1)_{\text{FN}}$	-	3	1	0	-	-	-	-	6

cation rules (see e.g. Refs. [26, 27]), lead to the Lagrangian

$$\begin{aligned} \mathcal{L}_Y = & \frac{y_e}{\Lambda} e^c (\varphi L) h_d + \frac{y_\mu}{\Lambda} \mu^c (\varphi L)' h_d + \frac{y_\tau}{\Lambda} \tau^c (\varphi L)'' h_d \\ & + \frac{x_a}{\Lambda^2} \xi (L h_u L h_u) + \frac{x_d}{\Lambda^2} (\varphi' L h_u L h_u) + \text{h.c.} + \dots, \end{aligned} \quad (11)$$

where Λ is the cut-off scale and the dots stand for higher dimensional operators. The notation is such that two fields a and b written as (ab) transform as $\underline{1}$, etc. If one chooses the real basis for A_4 , along with the flavon VEV alignments² $\langle \xi \rangle = u$, $\langle \varphi \rangle = (v, 0, 0)$ and $\langle \varphi' \rangle = (v', v', v')$, then the charged lepton mass matrix is diagonal, and the neutrino mass matrix

$$M_\nu = \frac{v_u^2}{\Lambda} \begin{pmatrix} a' + \frac{2d'}{3} & -\frac{d'}{3} & -\frac{d'}{3} \\ \cdot & \frac{2d'}{3} & a' - \frac{d'}{3} \\ \cdot & \cdot & \frac{2d'}{3} \end{pmatrix}, \quad (12)$$

is diagonalized by the TBM matrix,

$$U_{\text{TBM}} = \begin{pmatrix} \frac{2}{\sqrt{6}} & \frac{1}{\sqrt{3}} & 0 \\ -\frac{1}{\sqrt{6}} & \frac{1}{\sqrt{3}} & -\frac{1}{\sqrt{2}} \\ -\frac{1}{\sqrt{6}} & \frac{1}{\sqrt{3}} & \frac{1}{\sqrt{2}} \end{pmatrix}. \quad (13)$$

In this case M_ν is form-diagonalizable: the eigenvectors are independent of the parameters in the neutrino mass matrix. The charged lepton mass hierarchy is generated by the Froggatt-Nielsen (FN) mechanism: the $U(1)_{\text{FN}}$ charges 0, 1 and 3 are assigned to the right-handed charged singlets τ^c , μ^c and e^c , respectively, and a flavon θ that carries a negative unit of this charge is introduced, suppressing each mass term by powers of the small parameter

² Several methods have been proposed to explain the different alignments and solve the so-called "vacuum alignment problem"; these will not be discussed here. Note that we do not introduce more flavons to the original model, so that we can assume that the solution of the alignment problem will not be modified.

$\langle\theta\rangle/\Lambda \equiv \lambda < 1$. Explicitly,

$$m_\alpha = y_\alpha v_d \frac{v}{\Lambda} \lambda^{F_\alpha}, \quad (14)$$

where F_α is the relevant $U(1)_{\text{FN}}$ charge.

By assuming that (i) the Yukawa couplings y_α , x_a and x_d remain in a perturbative regime; (ii) the flavon VEVs are smaller than the cut-off scale and (iii) all flavon VEVs fall in approximately the same range, the authors of Ref. [39] obtain the relation

$$0.004 < \frac{v'}{\Lambda} \approx \frac{v}{\Lambda} \approx \frac{u}{\Lambda} < 1, \quad (15)$$

with the cut-off scale Λ ranging between 10^{12} and 10^{15} GeV, and $v_u \approx 174$ GeV.

In order to accommodate sterile neutrinos in this framework, we have added an additional sterile singlet, ν_s , transforming as $\underline{1}$ under A_4 and 1 under Z_3 . The A_4 invariant dimension-5 operator $\frac{1}{\Lambda}(\varphi' L h_u)\nu_s$ is not allowed by the Z_3 symmetry, and we are left with the terms

$$\mathcal{L}_{Y_s} = \frac{x_e}{\Lambda^2} \xi(\varphi' L h_u)\nu_s + \frac{x_f}{\Lambda^2} (\varphi' \varphi' L h_u)\nu_s + m_s \nu_s^c \nu_s^c + \text{h.c.}, \quad (16)$$

where m_s is a bare Majorana mass. As we will see, the chosen FN charge forces m_s to be at the desired eV scale. The modified 4×4 mass matrix is (cf. Eq. (12))

$$M_\nu^{4 \times 4} = \begin{pmatrix} a + \frac{2d}{3} & -\frac{d}{3} & -\frac{d}{3} & e \\ \cdot & \frac{2d}{3} & a - \frac{d}{3} & e \\ \cdot & \cdot & \frac{2d}{3} & e \\ \cdot & \cdot & \cdot & m_s \end{pmatrix}, \quad (17)$$

where $a = 2x_a \frac{uv_u^2}{\Lambda^2}$, $d = 2x_d \frac{v'v_u^2}{\Lambda^2}$ and $e = \sqrt{2}x_e \frac{uv'v_u}{\Lambda^2}$ have dimensions of mass. Note that the first three elements of the fourth row of $M_\nu^{4 \times 4}$ are identical because of the VEV alignment $\langle\varphi'\rangle = (v', v', v')$, which was necessary to generate TBM in the 3 neutrino case; this alignment combined with the A_4 multiplication rules also causes the second term in Eq. (16) (proportional to x_f) to vanish.

The correct mass scales can be obtained by assigning a $U(1)_{\text{FN}}$ charge of $F_{\nu_s} = 6$ to ν_s , in analogy to the mechanism used in the charged lepton sector. Indeed, in order to fit the data, the parameters a and d should be between 10^{-3} and 10^{-1} eV, the ratio $e/m_s \sim \mathcal{O}(10^{-1})$ to generate sufficient mixing, and $m_s \sim 1$ eV for the sterile neutrino mass.

As an explicit example, assume that $v'/\Lambda \approx v/\Lambda \approx u/\Lambda \simeq 10^{-1.5}$, in keeping with the constraints from Eq. (15), and that the cut-off scale is $\Lambda \simeq 10^{12.5}$ GeV. In this case one

obtains

$$\begin{aligned} a \sim d &\simeq 0.1 \left(\frac{u}{10^{11} \text{ GeV}} \right) \left(\frac{v_u}{10^2 \text{ GeV}} \right)^2 \left(\frac{10^{12.5} \text{ GeV}}{\Lambda} \right)^2 \text{ eV}, \\ e &\simeq 0.1 \left(\frac{\lambda}{10^{-1.5}} \right)^6 \left(\frac{u}{10^{11} \text{ GeV}} \right) \left(\frac{v'}{10^{11} \text{ GeV}} \right) \left(\frac{v_u}{10^2 \text{ GeV}} \right) \left(\frac{10^{12.5} \text{ GeV}}{\Lambda} \right)^2 \text{ eV}, \end{aligned} \quad (18)$$

with the assumption that the Yukawa couplings $x_{a,d,e}$ are of order 1, and that $\lambda \approx 10^{-1.5}$, so that $\langle \theta \rangle$ is in the same range as the other flavon VEVs.

The Majorana mass term $m_s \nu_s^c \nu_s^c$ is doubly suppressed by the $U(1)_{\text{FN}}$ charge, and there are additional terms which can give a contribution to this mass in addition to the bare term. From the particle assignments in Table II, the leading and next-to-leading order non-vanishing contributions to m_s are³

$$\left(\frac{x_s}{\Lambda} (\varphi \varphi) + \frac{x_{s'}}{\Lambda^2} \xi \xi \xi + \frac{x_{s''}}{\Lambda^2} (\varphi' \varphi') \xi \right) \nu_s^c \nu_s^c \implies \left(x_s \frac{v^2}{\Lambda} + x_{s'} \frac{u^3}{\Lambda^2} + x_{s''} \frac{3v'^2 u}{\Lambda^2} \right) \lambda^{2F_\nu}, \quad (19)$$

so that these terms are suppressed by λ^{12} , and the resulting Majorana mass can be of order eV, i.e.

$$m_s \simeq 10^{0.5} \left(\frac{\lambda}{10^{-1.5}} \right)^{12} \left(\frac{v}{10^{11} \text{ GeV}} \right)^2 \left(\frac{10^{12.5} \text{ GeV}}{\Lambda} \right) \text{ eV}. \quad (20)$$

In this case the contributions from the second and third terms in Eq. (19) are of order 0.1 eV, and do not affect the scale of m_s significantly. We conclude that the usual choice of scales and charges easily allows $a \sim d \sim e < m_s$ in $M_\nu^{4 \times 4}$ from Eq. (17).

Assuming that the parameters are all real, Eq. (17) is exactly diagonalized by

$$U = \begin{pmatrix} \frac{2}{\sqrt{6}} & \frac{1}{6e} \frac{K_-}{N_-} & 0 & \frac{1}{6e} \frac{K_+}{N_+} \\ -\frac{1}{\sqrt{6}} & \frac{1}{6e} \frac{K_-}{N_-} & -\frac{1}{\sqrt{2}} & \frac{1}{6e} \frac{K_+}{N_+} \\ -\frac{1}{\sqrt{6}} & \frac{1}{6e} \frac{K_-}{N_-} & \frac{1}{\sqrt{2}} & \frac{1}{6e} \frac{K_+}{N_+} \\ 0 & \frac{1}{N_-} & 0 & \frac{1}{N_+} \end{pmatrix}, \quad (21)$$

where $K_\pm = a - m_s \pm \sqrt{12e^2 + (a - m_s)^2}$ and $N_\pm^2 = 1 + \frac{(a - m_s \pm \sqrt{12e^2 + (a - m_s)^2})^2}{12e^2}$. If one assumes that $a < m_s$ and expands to second order in the small ratio e/m_s , the resulting

³ The term proportional to $\frac{x_{s'''}{\Lambda^2} (\varphi' \varphi' \varphi')$ vanishes after A_4 symmetry breaking.

mixing matrix is

$$U \simeq \begin{pmatrix} \frac{2}{\sqrt{6}} & \frac{1}{\sqrt{3}} & 0 & 0 \\ -\frac{1}{\sqrt{6}} & \frac{1}{\sqrt{3}} & -\frac{1}{\sqrt{2}} & 0 \\ -\frac{1}{\sqrt{6}} & \frac{1}{\sqrt{3}} & \frac{1}{\sqrt{2}} & 0 \\ 0 & 0 & 0 & 1 \end{pmatrix} + \begin{pmatrix} 0 & 0 & 0 & \frac{e}{m_s} \\ 0 & 0 & 0 & \frac{e}{m_s} \\ 0 & 0 & 0 & \frac{e}{m_s} \\ 0 & -\frac{\sqrt{3}e}{m_s} & 0 & 0 \end{pmatrix} + \begin{pmatrix} 0 & -\frac{\sqrt{3}e^2}{2m_s^2} & 0 & 0 \\ 0 & -\frac{\sqrt{3}e^2}{2m_s^2} & 0 & 0 \\ 0 & -\frac{\sqrt{3}e^2}{2m_s^2} & 0 & 0 \\ 0 & 0 & 0 & -\frac{3e^2}{2m_s^2} \end{pmatrix}, \quad (22)$$

giving the eigenvalues

$$m_1 = a + d, \quad m_2 = a - \frac{3e^2}{m_s}, \quad m_3 = -a + d, \quad m_4 = m_s + \frac{3e^2}{m_s}. \quad (23)$$

In this case one can see that $M_\nu^{4 \times 4}$ is not form-diagonalizable anymore: the second and fourth column of U are sensitive to the entries of $M_\nu^{4 \times 4}$. The mass-squared differences as well as the active-sterile mixing angles $\sin^2 \theta_{i4}$ ($i = 1, 2, 3$) are controlled by the four parameters in Eq. (17), with the mixing most sensitive to the ratio e/m_s . Note that both the normal and inverted orderings are allowed, in contrast to the standard three neutrino version of the model, which only allowed the normal ordering. By fitting the parameters a , d , e and m_s to the allowed range of the four parameters Δm_{S}^2 , Δm_{A}^2 , Δm_{41}^2 and $\sin^2 \theta_{14}$, we find that the masses are arbitrary, are not constrained to any particular region, and are in general uncorrelated with the mixing parameters. However, the lightest mass increases with $\sin^2 \theta_{14}$, which means that the effective mass in $0\nu\beta\beta$, $\langle m_{ee} \rangle \equiv |a + \frac{2d}{3}|$, also increases with $\sin^2 \theta_{14}$, as expected from Eq. (7). Figure 4 shows the allowed ranges of a, d, e . In general, a and d are approximately inversely proportional to each other.

Comparison of Eqs. (2) and (22), shows that $\sin \theta_{13} = 0$, i.e. this parameter retains its TBM value, whereas $\sin^2 \theta_{12}$ and $\sin^2 \theta_{23}$ receive small corrections:

$$\begin{aligned} \sin^2 \theta_{12} &= \frac{|U_{e2}|^2}{1 - |U_{e4}|^2} \simeq \frac{1}{3} \left[1 - 2 \left(\frac{e}{m_s} \right)^2 \right], \\ \sin^2 \theta_{23} &= \frac{|U_{\mu 3}|^2 (1 - |U_{e4}|^2)}{1 - |U_{e4}|^2 - |U_{\mu 4}|^2} \simeq \frac{1}{2} \left[1 + \left(\frac{e}{m_s} \right)^2 \right]. \end{aligned} \quad (24)$$

Note the correlation $\sin^2 \theta_{23} \simeq \frac{3}{4}(1 - \sin^2 \theta_{12})$ following from the above expressions. Other results of the model are $U_{s1} = U_{s3} = 0$ and $U_{e4} = U_{\mu 4} = U_{\tau 4}$. The three active-sterile mixing angles can be expressed in terms of the matrix elements U_{f4} as

$$\sin^2 \theta_{14} = |U_{e4}|^2, \quad \sin^2 \theta_{24} = \frac{|U_{\mu 4}|^2}{1 - |U_{e4}|^2}, \quad \sin^2 \theta_{34} = \frac{|U_{\tau 4}|^2}{1 - |U_{e4}|^2 - |U_{\mu 4}|^2}, \quad (25)$$

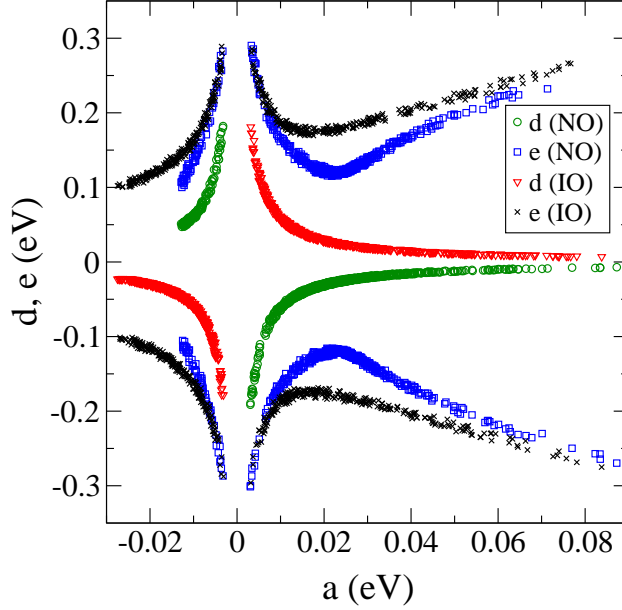


FIG. 4: The allowed values in $a - d$ and $a - e$ parameter space for normal (NO) and inverted (IO) ordering, obtained by varying each parameter between -0.5 and 0.5 eV, varying m_s between -1.5 and 1.5 eV, and requiring that the oscillation parameters lie in the correct range [7, 33].

and the model predicts them all to be of similar magnitude:

$$\sin^2\theta_{14} \simeq \sin^2\theta_{24} \simeq \sin^2\theta_{34} \simeq \left(\frac{e}{m_s}\right)^2 \simeq \frac{1}{2}(1 - 3\sin^2\theta_{12}) \simeq 2\sin^2\theta_{23} - 1, \quad (26)$$

to second order in the ratio e/m_s . The correlation (see Eqs. (24) and (26)) between the solar and atmospheric mixing parameters ($\sin^2\theta_{12}$ and $\sin^2\theta_{23}$) and the active-sterile mixing parameter ($\sin^2\theta_{14}$) is shown in Fig. 5, and is the same for both mass orderings.

Although this model appears to predict $\theta_{13} = 0$, this result depends on the triplet VEV alignments in the scalar sector. In the general case [40, 41], these alignments could be modified to $\langle\varphi\rangle = (v, v\epsilon_1^{\text{ch}}, v\epsilon_2^{\text{ch}})$ and $\langle\varphi'\rangle = (v', v'(1 + \epsilon_1), v'(1 + \epsilon_2))$, where the deviation parameters come from higher dimensional operators or renormalization group effects. Mixing angles will then receive corrections of the same order, proportional to $\epsilon_{1,2}^{\text{ch}}$ and $\epsilon_{1,2}$, so that one can accommodate the latest T2K result as well as the allowed range from Ref. [34]. These perturbations would also affect the fourth column of Eq. (17), thus altering the results in Eqs. (24) and (26).

We note here that the small mixing with sterile neutrinos will in general modify mixing scenarios. The mixing angles of active and sterile neutrinos are of order e/m_s , where e is any of the entries $(M_\nu^{4\times 4})_{fs}$ with $f = e, \mu, \tau$. Deviations from initial mixing angles $\theta_{12,13,23}$

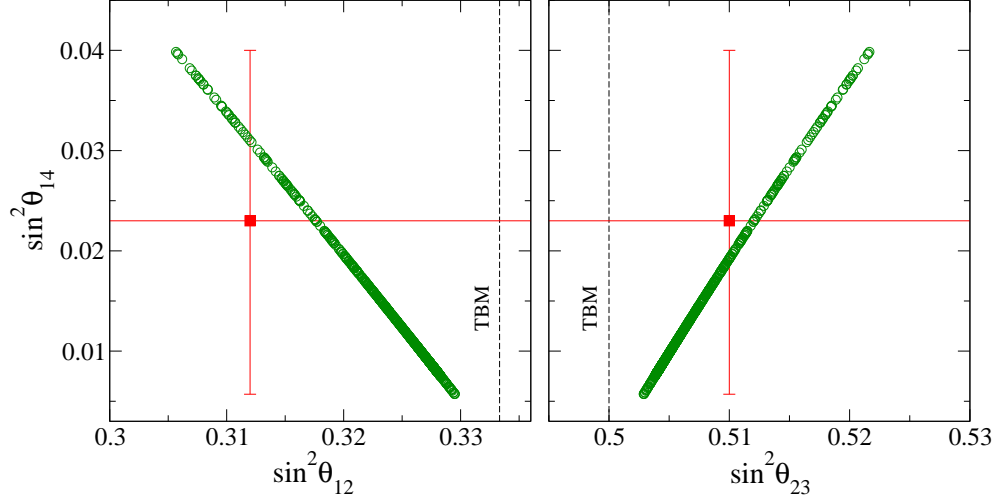


FIG. 5: $\sin^2\theta_{14}$ against $\sin^2\theta_{12}$ and $\sin^2\theta_{23}$, for both the normal and inverted ordering. The dashed (black) lines corresponds to the TBM values of $\sin^2\theta_{12}$ and $\sin^2\theta_{23}$, the solid (red) lines indicate the 2σ ranges of the parameters and the (red) square is the best-fit point [7, 33].

are then of the same order. The example we have discussed here has the particular feature that $U_{e4} = U_{\mu 4} = U_{\tau 4}$ and that the first and third row of U are identical to TBM. This will be different in other cases.

In a more general flavor symmetry context, it is instructive to note the origin of the eigenvector proportional to $(0, -1, 1, 0)^T$ in Eq. (22). This arises because of a generalized μ - τ symmetry. Consider an arbitrary 4×4 Majorana mass matrix $M_\nu^{4 \times 4}$. The defining matrix $P_{\mu\tau}$ for the Z_2 corresponding to μ - τ symmetry fulfills $P_{\mu\tau}^2 = \mathbb{1}$ and the invariance condition $P_{\mu\tau} M_\nu^{4 \times 4} P_{\mu\tau} = M_\nu^{4 \times 4}$, so that $P_{\mu\tau}$ and the resulting mass matrix are given by

$$P_{\mu\tau} = \begin{pmatrix} 1 & 0 & 0 & 0 \\ 0 & 0 & 1 & 0 \\ 0 & 1 & 0 & 0 \\ 0 & 0 & 0 & 1 \end{pmatrix} \quad \text{and} \quad M_\nu^{4 \times 4} = \begin{pmatrix} \tilde{a} & \tilde{b} & \tilde{b} & \tilde{d} \\ \cdot & \tilde{e} & \tilde{f} & \tilde{g} \\ \cdot & \cdot & \tilde{e} & \tilde{g} \\ \cdot & \cdot & \cdot & \tilde{m} \end{pmatrix}. \quad (27)$$

The eigenvalue $\tilde{e} - \tilde{f}$ of this mass matrix corresponds to an eigenvector proportional to $(0, -1, 1, 0)^T$. This Z_2 invariance, usually present in A_4 models [26], arises by spontaneous A_4 breaking. Regarding the nearly TBM mixing, there is a second Z_2 under which $M_\nu^{4 \times 4}$ is

invariant. It is defined by the generator

$$P_{\text{sol}} = \frac{1}{3} \begin{pmatrix} -1 & 2 & 2 & 0 \\ 2 & -1 & 2 & 0 \\ 2 & 2 & -1 & 0 \\ 0 & 0 & 0 & 3 \end{pmatrix}. \quad (28)$$

Additional invariance under this Z_2 (note that $P_{\mu\tau}$ and P_{sol} commute) requires $\tilde{f} = \tilde{a} - \tilde{e} + \tilde{b}$ and $\tilde{d} = \tilde{g}$. As a result, the eigenvalue $2\tilde{e} - \tilde{b} - \tilde{a}$ has an eigenvector proportional to $(-2, 1, 1, 0)^T$. Furthermore, it holds that $U_{es} = U_{\mu s} = U_{\tau s}$. The main features of Eq. (17) are therefore explained by the two Z_2 symmetries. In addition, the simplicity of the A_4 model leads to $\tilde{e} = -2\tilde{b}$, but does not modify the mixing properties that arise from the two Z_2 symmetries.

Let us denote with S the upper left 3×3 part of P_{sol} . With a suitably chosen diagonal phase matrix $T = \text{diag}(1, e^{-i2\pi/3}, e^{i2\pi/3})$, under which the charged lepton mass matrix $M_\ell M_\ell^\dagger$ is invariant, it holds that $T^3 = (ST)^3 = \mathbb{1}$. Hence, S and T generate A_4 , and the charged lepton Z_3 defined by T arises again by spontaneous A_4 breaking. These well known features [26] of A_4 models are not altered by our modification.

B. Two sterile neutrinos

In order to have two sterile neutrinos in the A_4 model, one can simply add a second sterile singlet ν_{s_2} . As before, this sterile neutrino is a singlet $\underline{1}$ under A_4 and 1 under Z_3 , and carries the $U(1)_{\text{FN}}$ charge $F_{\nu_s} = 6$. With the additional assumption that the sterile sector of the mass matrix is diagonal⁴, the symmetric 5×5 mass matrix is

$$M_\nu^{5 \times 5} = \begin{pmatrix} a + \frac{2d}{3} & -\frac{d}{3} & -\frac{d}{3} & e & f \\ \cdot & \frac{2d}{3} & a - \frac{d}{3} & e & f \\ \cdot & \cdot & \frac{2d}{3} & e & f \\ \cdot & \cdot & \cdot & m_{s_1} & 0 \\ \cdot & \cdot & \cdot & \cdot & m_{s_2} \end{pmatrix}. \quad (29)$$

Similar statements about the Z_2 invariance of properly extended $P_{\mu\tau}$ and P_{sol} symmetries can be made here (see the discussion at the end of the last subsection). Since f and m_{s_2} arise in analogy to e and m_s in the one sterile neutrino case, we expect that e and f , as well as m_{s_1} and m_{s_2} , are each of similar magnitude, respectively. In analogy to the case

⁴ This can be achieved, for example, with an additional discrete symmetry such as Z_2 operating only in the sterile sector.

discussed in the previous subsection, the mass matrix is approximately diagonalized by

$$\begin{aligned}
U = & \begin{pmatrix} \frac{2}{\sqrt{6}} & \frac{1}{\sqrt{3}} & 0 & 0 & 0 \\ -\frac{1}{\sqrt{6}} & \frac{1}{\sqrt{3}} & -\frac{1}{\sqrt{2}} & 0 & 0 \\ -\frac{1}{\sqrt{6}} & \frac{1}{\sqrt{3}} & \frac{1}{\sqrt{2}} & 0 & 0 \\ 0 & 0 & 0 & 1 & 0 \\ 0 & 0 & 0 & 0 & 1 \end{pmatrix} + \begin{pmatrix} 0 & 0 & 0 & \frac{e}{m_{s_1}} & \frac{f}{m_{s_2}} \\ 0 & 0 & 0 & \frac{e}{m_{s_1}} & \frac{f}{m_{s_2}} \\ 0 & 0 & 0 & \frac{e}{m_{s_1}} & \frac{f}{m_{s_2}} \\ 0 & -\frac{\sqrt{3}e}{m_{s_1}} & 0 & 0 & 0 \\ 0 & -\frac{\sqrt{3}f}{m_{s_2}} & 0 & 0 & 0 \end{pmatrix} \\
& + \begin{pmatrix} 0 & -\frac{\sqrt{3}}{2} \left(\frac{e^2}{m_{s_1}^2} + \frac{f^2}{m_{s_2}^2} \right) & 0 & 0 & 0 \\ 0 & -\frac{\sqrt{3}}{2} \left(\frac{e^2}{m_{s_1}^2} + \frac{f^2}{m_{s_2}^2} \right) & 0 & 0 & 0 \\ 0 & -\frac{\sqrt{3}}{2} \left(\frac{e^2}{m_{s_1}^2} + \frac{f^2}{m_{s_2}^2} \right) & 0 & 0 & 0 \\ 0 & 0 & 0 & -\frac{3e^2}{2m_{s_1}^2} & -\frac{3ef}{2m_{s_1}m_{s_2}} \\ 0 & 0 & 0 & -\frac{3ef}{2m_{s_1}m_{s_2}} & -\frac{3f^2}{2m_{s_2}^2} \end{pmatrix}, \tag{30}
\end{aligned}$$

assuming that $a < m_{s_{1,2}}$ and that the ratios e/m_{s_1} and f/m_{s_2} are small. The mass eigenvalues are

$$m_1 = a + d, \quad m_2 = a - \frac{3e^2}{m_{s_1}} - \frac{3f^2}{m_{s_2}}, \quad m_3 = -a + d, \quad m_4 = m_{s_1} + \frac{3e^2}{m_{s_1}}, \quad m_5 = m_{s_2} + \frac{3f^2}{m_{s_2}}, \tag{31}$$

to second order in the ratios e/m_{s_1} and f/m_{s_2} .

Once again, the reactor mixing angle retains its TBM value, and the predictions for $\sin^2\theta_{12}$ and $\sin^2\theta_{23}$ are

$$\begin{aligned}
\sin^2\theta_{12} &\simeq \frac{1}{3} \left[1 - 2 \left(\left(\frac{e}{m_{s_1}} \right)^2 + \left(\frac{f}{m_{s_2}} \right)^2 \right) \right], \\
\sin^2\theta_{23} &\simeq \frac{1}{2} \left[1 + \left(\frac{e}{m_{s_1}} \right)^2 + \left(\frac{f}{m_{s_2}} \right)^2 \right], \tag{32}
\end{aligned}$$

in analogy to the 4×4 case. Using the explicit parameterization (5) of the 5×5 mixing matrix, the six active-sterile mixing angles can be approximated by

$$\sin^2\theta_{i4} \simeq \left(\frac{e}{m_{s_1}} \right)^2, \quad \sin^2\theta_{i5} \simeq \left(\frac{f}{m_{s_2}} \right)^2 \quad (i = 1, 2, 3), \tag{33}$$

with the additional assumption that U is real.

Note that without an additional discrete symmetry the sterile sector of Eq. (29) would be a 2×2 democratic matrix with entries of order $m_{s_1} \simeq m_{s_2} \simeq 1$ eV. In this case the active-sterile mixing would be modified by the presence of an additional large 4-5 rotation in the overall 5×5 mixing matrix.

IV. REALIZATION OF LIGHT STERILE NEUTRINOS IN SEESAW MODELS

We now discuss how one can accommodate eV-scale sterile neutrinos in seesaw frameworks. We start from the simplest type I seesaw scenario and then present an interesting extension to this.

A. Sterile neutrinos from type I seesaw

In the canonical type I seesaw model, three heavy right-handed neutrinos $\nu_R = (\nu_{R1}, \nu_{R2}, \nu_{R3})$ are introduced and the neutrino mass Lagrangian reads

$$-\mathcal{L}_m = \overline{\nu}_L M_D \nu_R + \frac{1}{2} \overline{\nu}_R^c M_R \nu_R + \text{h.c.}, \quad (34)$$

where the Dirac mass matrix M_D is an arbitrary matrix, while M_R is symmetric according to the Majorana nature of right-handed neutrinos. In the basis (ν_L, ν_R^c) , the neutrino mass matrix is a 6×6 matrix:

$$M_\nu = \begin{pmatrix} 0 & M_D \\ M_D^T & M_R \end{pmatrix}, \quad (35)$$

and if the entries of M_D are all much smaller than the eigenvalues of M_R , light neutrinos acquire masses after the heavy right-handed neutrinos are integrated out, *viz.*

$$m_\nu \simeq -M_D M_R^{-1} M_D^T. \quad (36)$$

The mixing between heavy and light neutrinos comes from the full diagonalization of M_ν , and is approximately given by

$$R \simeq M_D M_R^{-1}, \quad (37)$$

in the basis where M_R is diagonal. The non-unitary mixing matrix relating the light neutrino flavor eigenstates and their mass eigenstates is modified to

$$V \simeq (1 - \frac{1}{2} R R^\dagger) U, \quad (38)$$

where U is a unitary matrix satisfying $U^\dagger m_\nu U^* = \text{diag}(m_1, m_2, m_3)$. Thus, in principle the type I seesaw mechanism predicts sterile neutrinos mixed with active neutrinos. However, with M_D naturally located at the electroweak scale of 10^2 GeV and from the requirement of sub-eV light neutrino masses, one typically has that $M_R \sim 10^{14}$ GeV. The mass and mixing parameters are therefore not suited to explain eV-scale light neutrinos. Possible ways out of this dilemma are (i) to lower the overall seesaw scale down to $M_R \sim \text{eV}$ [42]; or (ii) bring

one of the heavy neutrinos and the Dirac mass matrix entries associated with it down to the eV scale. This is in the spirit of the ν MSM [43], where however the adjective “light” denotes keV sterile neutrinos, which can act as warm dark matter particles.

In the first case, one may use for instance $M_R \simeq 1.5$ eV and $M_D \simeq 0.3$ eV, for which the light neutrino mass scale lies around 0.06 eV and $R \simeq 0.2$ according to Eqs. (36) and (37). This is roughly in agreement with the recently reported range of sterile neutrinos from the reactor anti-neutrino anomaly. One would expect three sterile neutrinos in this case. In this scenario, there is no neutrino-less double beta decay, since both the active and sterile neutrinos contribute to the effective mass $\langle m_{ee} \rangle$, and their contributions are exactly cancelled [42]. This is a consequence of the zero in the upper left entry of Eq. (35) and the fact that all six neutrino masses are below 100 MeV, which is the typical momentum exchange in $0\nu\beta\beta$. In addition, neither the baryon asymmetry problem nor the dark matter problem is solved in this framework, since the sterile neutrinos are too light. It is also questionable why M_D should be so tiny compared to the weak scale, since both arise from Yukawa couplings to the SM Higgs doublet.

Consider now the second possibility, namely bringing one right-handed neutrino down to the eV scale. In order to simultaneously explain the baryon asymmetry of the Universe and the reactor anomaly, a minimal extension of the SM requires at least one light right-handed (sterile) neutrino ν_s together with two heavy right-handed neutrinos (ν_{R1} and ν_{R2}). In this case, the Lagrangian for neutrino masses is

$$-\mathcal{L}_m = \overline{\nu}_L M_D \nu_R + \overline{\nu}_L M_S \nu_s + \frac{1}{2} \overline{\nu}_R^c M_R \nu_R + \frac{1}{2} \overline{\nu}_S^c \mu_S \nu_S + \text{h.c.}, \quad (39)$$

where M_D , M_R and M_S are 3×2 , 2×2 and 3×1 mass matrices, respectively. The full neutrino mass matrix in the basis $(\nu_L, \nu_s^c, \nu_R^c)$ reads

$$M_\nu = \begin{pmatrix} 0 & 0 & 0 & (M_S)_{11} & (M_D)_{11} & (M_D)_{12} \\ 0 & 0 & 0 & (M_S)_{21} & (M_D)_{21} & (M_D)_{22} \\ 0 & 0 & 0 & (M_S)_{31} & (M_D)_{31} & (M_D)_{32} \\ (M_S)_{11} & (M_S)_{21} & (M_S)_{31} & \mu_S & 0 & 0 \\ (M_D)_{11} & (M_D)_{21} & (M_D)_{31} & 0 & M_1 & 0 \\ (M_D)_{12} & (M_D)_{22} & (M_D)_{32} & 0 & 0 & M_2 \end{pmatrix}, \quad (40)$$

where we work in the basis where M_R is diagonal (this is always possible by performing a proper basis transformation).

We assume that two of the right-handed neutrinos are heavy (e.g. above the TeV scale or higher) and μ_S is much smaller than M_R , i.e. around the eV scale. Then, at energy scales much lower than M_R , ν_{Ri} should be decoupled from the full theory, and one obtains a 4×4

matrix for active and sterile neutrinos, *viz.*

$$M_\nu^{4 \times 4} = \begin{pmatrix} -M_D M_R^{-1} M_D^T & M_S \\ M_S^T & \mu_S \end{pmatrix}. \quad (41)$$

In the case where $\mu_S \gg M_S$, one may apply the seesaw formula once again, and arrive at the light neutrino mass matrix

$$m_\nu \simeq -M_D M_R^{-1} M_D^T - M_S \mu_S^{-1} M_S^T. \quad (42)$$

The mixing between active and sterile neutrinos is characterized by $R = M_S \mu_S^{-1}$. Comparison with Eq. (2) gives

$$\sin \theta_{14} \simeq (M_S)_{11} \mu_S^{-1}, \quad (43)$$

together with the mass of the sterile neutrino

$$m_s \simeq \mu_S. \quad (44)$$

The scenario under discussion permits neutrino-less double beta decay, since the active and sterile neutrino contributions do not cancel with each other. Furthermore, in this scenario the baryon asymmetry of the Universe can be explained via the leptogenesis mechanism, for which at least two heavy right-handed neutrinos are required. However, it should also be noticed that none of the singlet neutrinos have masses in the allowed range of sterile neutrino warm dark matter (i.e. around keV), so that one cannot simultaneously solve the dark matter puzzle [43].

The question arises how to make one of the right-handed neutrinos so light compared to the other two. One obvious possibility is to start with a flavor symmetry that predicts one of the masses to be zero. Small breaking of the symmetry will then generate a small but non-zero mass. This simple idea has been pursued in the context of keV dark matter [44, 45], and will work for light sterile neutrinos as well. One possible symmetry that can be used is $L_e - L_\mu - L_\tau$ [46, 47].

B. Minimal extended type I seesaw

The cases discussed in the last subsection have the feature that the fundamental seesaw Lagrangian already contains at least one particle at the desired eV scale. This is somewhat contradictory to the seesaw spirit, and one may ask whether it is also possible to generate eV-scale sterile neutrinos without the *a priori* presence of such states.

Here we consider an interesting extension of the type I seesaw model, in which three right-handed neutrinos together with *one* singlet S are introduced. A similar idea was used

in Ref. [48], with a sterile state of mass $\sim 10^{-3}$ eV introduced in order to explain the solar neutrino problem. Here we will show that there is a natural eV-scale sterile neutrino in this scenario, without the need of inserting a small mass term for ν_s . The Lagrangian of this scenario is given by

$$-\mathcal{L}_m = \overline{\nu}_L M_D \nu_R + \overline{S^c} M_S \nu_R + \frac{1}{2} \overline{\nu_R^c} M_R \nu_R + \text{h.c.}, \quad (45)$$

where M_S is a 1×3 matrix. The full 7×7 neutrino mass matrix in the basis (ν_L, ν_R^c, S^c) reads

$$M_\nu^{7 \times 7} = \begin{pmatrix} 0 & M_D & 0 \\ M_D^T & M_R & M_S^T \\ 0 & M_S & 0 \end{pmatrix}. \quad (46)$$

In the case where $M_R \gg M_S > M_D$, one should first decouple heavy right-handed neutrinos using the canonical seesaw formula, and the effective neutrino mass matrix in the basis (ν_L, S^c) is given by

$$M_\nu^{4 \times 4} = - \begin{pmatrix} M_D M_R^{-1} M_D^T & M_D M_R^{-1} M_S^T \\ M_S (M_R^{-1})^T M_D^T & M_S M_R^{-1} M_S^T \end{pmatrix}. \quad (47)$$

Since M_S is larger than M_D by definition, one can apply the seesaw formula once again and obtain

$$m_\nu \simeq M_D M_R^{-1} M_S^T (M_S M_R^{-1} M_S^T)^{-1} M_S (M_R^{-1})^T M_D^T - M_D M_R^{-1} M_D^T, \quad (48)$$

for the active neutrinos, whereas there exists one sterile neutrino with mass

$$m_s \simeq -M_S M_R^{-1} M_S^T. \quad (49)$$

Note that the right-hand-side of Eq. (48) does not vanish since M_S is a vector rather than a square matrix; if M_S were a square matrix this would lead to an exact cancellation between the two terms of Eq. (48).

The active-sterile neutrino mixing matrix takes a 4×4 form, i.e.,

$$V \simeq \begin{pmatrix} (1 - \frac{1}{2} R R^\dagger) U & R \\ -R^\dagger U & 1 - \frac{1}{2} R^\dagger R \end{pmatrix}, \quad (50)$$

where $R = M_D M_R^{-1} M_S^T (M_S M_R^{-1} M_S^T)^{-1}$. Essentially, V_{14} (i.e. $\sin \theta_{14}$) is suppressed by the ratio $\mathcal{O}(M_D/M_S)$.

As a naive numerical example, for $M_D \simeq 100$ GeV, $M_S \simeq 500$ GeV and

$M_R \simeq 2 \times 10^{14}$ GeV, one may estimate that $m_\nu \simeq 0.05$ eV, $m_s \simeq 1.3$ eV together with $R \simeq 0.2$. This is in very good agreement with the fitted sterile neutrino parameters from Table I. Neutrino-less double beta decay is again allowed because not all of the neutrinos are light.

Note that one of the light neutrinos is massless since the rank of $M_\nu^{4 \times 4}$ is three. This model is a minimal extension of the type I seesaw in the sense that one needs at least three heavy neutrinos to suppress the masses of both active and sterile neutrinos. In other words, two heavy right-handed neutrinos give rise to two massive active neutrinos, while the other one is responsible for the mass of ν_s .

Unfortunately, if we embed this scenario into a grand unified theory framework it cannot be gauge anomaly free since we have only one generation of S . It is also not possible to accommodate two eV-scale sterile neutrinos in this scenario, unless the number of heavy neutrinos is increased. Apart from these shortcomings, the scenario possesses the following features:

- apart from the electroweak and seesaw scales, one does not artificially insert small mass scales for sterile neutrino masses. As in the canonical type I seesaw, one can take $M_S > M_D \sim \mathcal{O}(10^2 \text{ GeV})$, while M_R can be chosen close to the $B - L$ scale, not far from the grand unification scale;
- it is a minimal extension of the type I seesaw since three heavy right-handed neutrinos can lead to at most three massive light neutrinos (the “seesaw-fair-play-rule” [49]), out of which two are active and needed to account for the solar and atmospheric neutrino mixing. It is more predictive owing to the absence of one active neutrino mass, while it still accommodates all the experimental data;
- there exist heavy right-handed neutrinos that could be responsible for thermal leptogenesis. Note that, in the setup we considered, right-handed neutrinos would preferably decay to the sterile neutrino since their coupling to S is larger than that to active neutrinos. However, this drawback could be circumvented since S enters in the one-loop self-energy diagram of the decay of right-handed neutrinos, which could compensate for this.

In this section we have exclusively used the type I seesaw and an extension of it. We note that type II seesaw does not provide the possibility of light sterile neutrinos, due to the absence of fermionic degrees of freedom. Type III seesaw is formally analogous to type I, because the neutral components of the fermion triplets play the role of heavy neutrinos. However, these components are not gauge singlets.

V. CONCLUSION

Motivated by recently reported hints for sterile neutrinos from particle physics, astroparticle physics and cosmology, we have studied the realization of light eV-scale sterile neutrinos in both model-independent and -dependent manners. The phenomenological consequences of light sterile neutrinos were discussed and we pointed out that the presence of such light sterile neutrinos would significantly change the oscillation probabilities in short-baseline experiments as well as the effective mass measured in neutrino-less double beta decay experiments. It turns out that the sterile contributions to the effective mass could lead to a vanishing $\langle m_{ee} \rangle$ even if the three active neutrinos obey an inverted ordering, which is clearly different from the predictions of the standard picture of three active neutrinos. Scenarios in which the sterile states are heavier than the active ones are safest in what regards cosmological mass limits; the other cases turn out to have rather large contributions, and are even in danger of being ruled out by current limits on the effective mass.

We then focused on the possibility of embedding sterile neutrinos into an effective theory with the A_4 flavor symmetry, and showed the corrections to the TBM pattern that result from this. We found that light sterile neutrinos can naturally be accommodated in the flavor A_4 symmetry, and their mixing with active neutrinos is correlated to the deviation from exact TBM. The departure from the initial mixing scheme is a general feature of such approaches; we only studied one example in detail. Furthermore, we have shown that light sterile neutrinos can be realized in extensions of the seesaw model. Regardless of naturalness, the type I seesaw with three right-handed neutrinos could, in principle, provide candidates for light sterile neutrinos. Besides the type I seesaw framework, we have presented a minimal extended type I seesaw model, in which, without the need of introducing tiny Yukawa couplings, the smallness of sterile neutrino masses is ascribed to the existence of heavy singlet neutrinos, whereas the mixing between active and sterile neutrinos could still be sizable. Note that all of the models we have discussed share the feature that the sterile neutrinos are heavier than the active ones.

As mentioned before, we only concentrate on eV-scale sterile neutrinos in the current study. In general, a keV sterile neutrino, which may lead to rich phenomenological consequences in the early Universe and supernova explosions, could also be accommodated in the models discussed in this work. A detailed survey could be useful and will be elaborated on in future.

Acknowledgments

This work was supported by the ERC under the Starting Grant MANITOP and by the Deutsche Forschungsgemeinschaft in the Transregio 27 “Neutrinos and beyond – weakly interacting particles in physics, astrophysics and cosmology”. JB thanks M. Holthausen,

K.L. McDonald and T. Schwetz for useful discussions.

Appendix A: Short-baseline neutrino oscillations: 3+2/2+3 vs. 1+3+1

When neutrinos propagate in vacuum, the probability of finding a neutrino of initial flavor α in the flavor state β at the baseline L is given by

$$P_{\alpha\beta} = |\langle \nu_\beta(L) | \nu_\alpha(0) \rangle|^2 = \left| \sum_i U_{\beta i} U_{\alpha i}^* e^{-iE_i L} \right|^2 \quad (\text{A-1})$$

$$= \delta_{\alpha\beta} - 4 \sum_{i>j} \text{Re} (U_{\alpha i}^* U_{\alpha j} U_{\beta i} U_{\beta j}^*) \sin^2 \left(\frac{\Delta_{ij} L}{4E} \right) + 2 \sum_{i>j} \text{Im} (U_{\alpha i}^* U_{\alpha j} U_{\beta i} U_{\beta j}^*) \sin \left(\frac{\Delta_{ij} L}{2E} \right),$$

where $\Delta_{ij} = m_i^2 - m_j^2$. The current global-fit of neutrino oscillation experiments indicates that (at 2σ) $\Delta m_{21}^2 \equiv \Delta_{21} = (7.24 \dots 7.99) \times 10^{-5} \text{ eV}^2$ and $\Delta m_{31}^2 \equiv |\Delta_{31}| = (2.17 \dots 2.64) \times 10^{-3} \text{ eV}^2$ and that the corresponding mixing angles are $\sin^2 \theta_{12} = 0.28 \dots 0.35$, $\sin^2 \theta_{23} = 0.41 \dots 0.61$ and $\sin^2 \theta_{13} < 0.031$ [33], where we have neglected small differences between normal and inverted ordering, which are irrelevant for our discussion. The parameters associated with sterile states are given in Table I. The oscillation probability for anti-neutrinos can be simply obtained from Eq. (A-1) by the replacement $U \rightarrow U^*$.

It should be stressed that for a terrestrial based neutrino oscillation experiment the baseline length is usually fixed, which allows one to make reasonable expansions of the oscillation probabilities. In a reactor anti-neutrino oscillation experiment, e.g. Double Chooz or Daya Bay, the detector is typically located at a baseline of around 1 km, while the average energy of neutrinos is $\bar{E} \sim 4 \text{ MeV}$. One can thus estimate that $L/E \sim \mathcal{O}(10^3) \text{ eV}^{-2}$, indicating that the oscillation term containing Δ_{21} can be safely ignored. In addition, the oscillation frequency related to the mass-squared difference Δ_{4i} (Δ_{5i}) is much smaller than the baseline, and thus the Δ_{4i} (Δ_{5i}) term generates a fast oscillation. The anti-neutrino survival probability then approximates to

$$P_{\bar{\nu}_e \rightarrow \bar{\nu}_e} \simeq 1 - 2 |U_{e4}|^2 - 4 |U_{e3}|^2 \sin^2 \left(\frac{\Delta_{31} L}{4E} \right)$$

$$= 1 - 2 \sin^2 \theta_{14} - \cos^4 \theta_{14} \sin^2 (2\theta_{13}) \sin^2 \left(\frac{\Delta_{31} L}{4E} \right), \quad (\text{A-2})$$

for the case of one sterile neutrino (1+3 and 3+1), and

$$P_{\bar{\nu}_e \rightarrow \bar{\nu}_e} \simeq 1 - 2 |U_{e4}|^2 - 2 |U_{e5}|^2 - 4 |U_{e3}|^2 \sin^2 \left(\frac{\Delta_{31} L}{4E} \right), \quad (\text{A-3})$$

for the case of two sterile neutrinos (3+2, 2+3 and 1+3+1). It is clearly seen that the effect of the sterile neutrino(s) is merely to reduce the total neutrino flux, which is needed to explain

the recently reported reactor anti-neutrino anomaly. Note that if in the Double Chooz experiment the neutrino flux is calibrated using the near detector instead of a Monte Carlo simulation, the total shift of the neutrino flux is cancelled when comparing the number of events in the near and far detectors, thus having no effect on the measurement of θ_{13} .

In order to observe the oscillation effects induced by sterile neutrinos at a reactor neutrino experiment, a very short baseline, e.g., $L \sim \mathcal{O}(10 \text{ m})$, turns out to be very attractive. At such a short baseline length, the Δ_{31} contributions to the oscillation probability can be neglected, and the survival probability reads

$$P_{\bar{\nu}_e \rightarrow \bar{\nu}_e} \simeq 1 - 4|U_{e4}|^2 \sin^2 \left(\frac{\Delta_{41} L}{4E} \right) = 1 - \sin^2(2\theta_{14}) \sin^2 \left(\frac{\Delta_{41} L}{4E} \right), \quad (\text{A-4})$$

for the 3+1/1+3 case, and

$$P_{\bar{\nu}_e \rightarrow \bar{\nu}_e} \simeq 1 - 4|U_{e4}|^2 \sin^2 \left(\frac{\Delta_{41} L}{4E} \right) - 4|U_{e5}|^2 \sin^2 \left(\frac{\Delta_{51} L}{4E} \right), \quad (\text{A-5})$$

for the 2+3, 3+2 or 1+3+1 cases. Note that the oscillation term proportional to $\sin^2 \left(\frac{\Delta_{54} L}{4E} \right)$ is suppressed by a factor $|U_{e4} U_{e5}|^2$, and can hence be neglected. The practical realization of a detector so close to a reactor is not straightforward, and will not be discussed here (see Ref. [50] for a recent proposal). So far there is no possibility to distinguish 2+3/3+2 from 1+3+1 scenarios.

The LSND and MiniBooNE experiments report an excess of electron anti-neutrino events in the oscillation channel $\bar{\nu}_\mu \rightarrow \bar{\nu}_e$, with a baseline and energy setup $L/E \sim \mathcal{O}(1) \text{ eV}^{-2}$. In analogy to the very short baseline reactor neutrino oscillations, the oscillation term related to Δ_{31} can be ignored, and the transition probability reads

$$P_{\bar{\nu}_\mu \rightarrow \bar{\nu}_e} \simeq 4|U_{e4}|^2 |U_{\mu 4}|^2 \sin^2 \left(\frac{\Delta_{41} L}{4E} \right), \quad (\text{A-6})$$

for the 3+1/1+3 case, and

$$\begin{aligned} P_{\bar{\nu}_\mu \rightarrow \bar{\nu}_e} \simeq & 4|U_{e4}|^2 |U_{\mu 4}|^2 \sin^2 \left(\frac{\Delta_{41} L}{4E} \right) + 4|U_{e5}|^2 |U_{\mu 5}|^2 \sin^2 \left(\frac{\Delta_{51} L}{4E} \right) \\ & + 8|U_{e4} U_{\mu 4} U_{e5} U_{\mu 5}| \sin \left(\frac{\Delta_{41} L}{4E} \right) \sin \left(\frac{\Delta_{51} L}{4E} \right) \cos \left(\frac{\Delta_{54} L}{4E} + \delta \right), \end{aligned} \quad (\text{A-7})$$

for the five neutrino case with $\delta \equiv \arg(U_{e4}^* U_{\mu 4} U_{e5} U_{\mu 5}^*) \simeq \delta_{14} - \delta_{24} - \delta_{15}$, where we have given the phase in the explicit parameterization of Eq. (5). The additional CP violating phase in Eq. (A-7) leads to a CP asymmetry in the transition probability between the neutrino and anti-neutrino modes, which is of particular interest in view of the null oscillation results from the neutrino running of MiniBooNE. In addition, the last term of Eq. (A-7) indicates

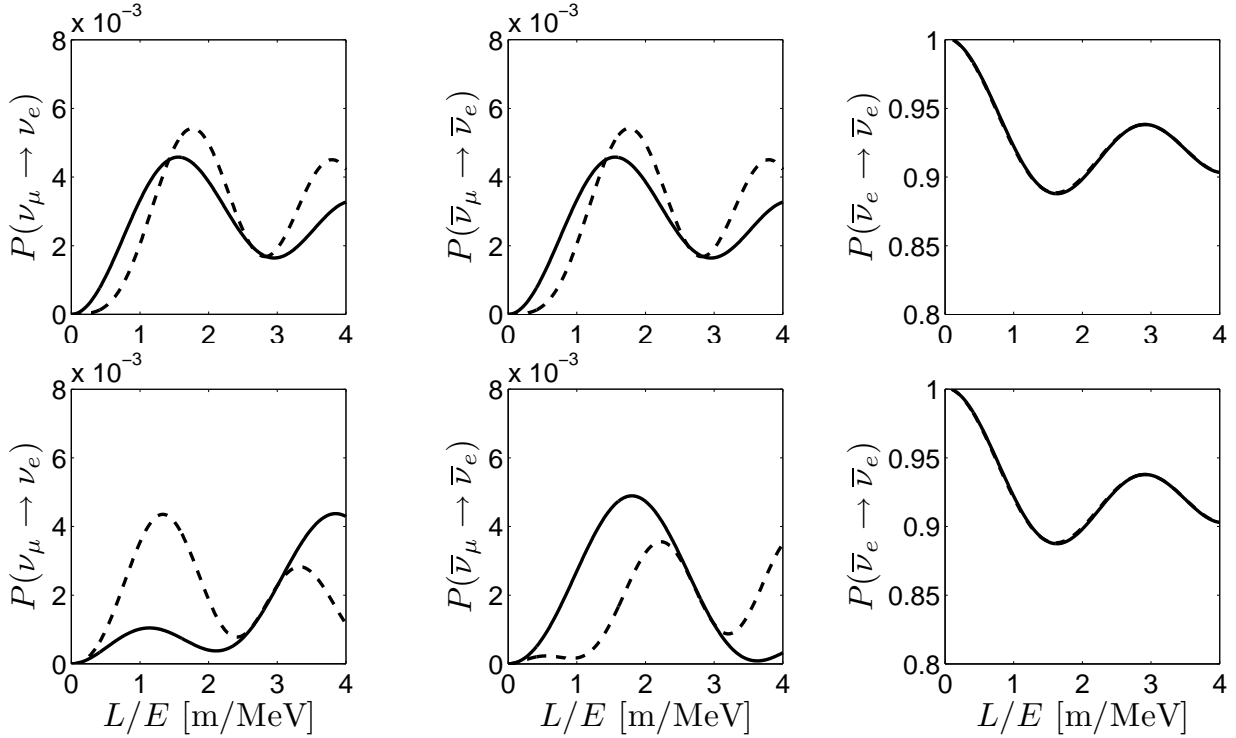


FIG. 6: The oscillation probabilities with respect to the quantity L/E in the 3+2/2+3 cases (solid lines) and 1+3+1 case (dashed lines). The mixing parameters are the best-fit values from TABLE II of Ref. [33] and TABLE II of Ref. [7]. In the upper panel, we set all CP violating phases to be zero, whereas in the lower panel $\delta = \frac{\pi}{2}$ is assumed.

a distinctive difference between the 3+2/2+3 and 1+3+1 cases due to the presence of Δ_{54} . Explicitly, in the 3+2/2+3 cases one has $\Delta_{54} = |\Delta_{51}| - |\Delta_{41}|$ whereas in the 1+3+1 case, $\Delta_{54} \simeq |\Delta_{51}| + |\Delta_{41}|$, which changes the transition probability regardless of the choice of CP violating phases.

We illustrate the oscillation probabilities with respect to the ratio L/E in Fig. 6 for the 3+2/2+3 and 1+3+1 cases. It is clear that the transition probabilities are quite different in the hierarchy schemes, whereas the survival probability is not sensitive to the sterile neutrino hierarchies since the Δ_{54} contributions are suppressed. Furthermore, if non-vanishing CP violating phases are included there are visible differences between neutrino and anti-neutrino flavor transitions, implying that a detector at very short distance would be an ideal place to search for the CP violation related to sterile neutrinos.

-
- [1] M. Gonzalez-Garcia and M. Maltoni, Phys. Rept. **460**, 1 (2008), 0704.1800.
 - [2] M. Sorel, J. M. Conrad, and M. Shaevitz, Phys. Rev. **D 70**, 073004 (2004), hep-ph/0305255.
 - [3] M. Maltoni and T. Schwetz, Phys. Rev. **D 76**, 093005 (2007), 0705.0107.
 - [4] G. Karagiorgi, Z. Djurcic, J. Conrad, M. Shaevitz, and M. Sorel, Phys. Rev. **D 80**, 073001

- (2009), 0906.1997.
- [5] C. Giunti and M. Laveder, Phys. Rev. **D 82**, 053005 (2010), 1005.4599.
 - [6] G. Mention, M. Fechner, T. Lasserre, T. Mueller, D. Lhuillier, et al., Phys. Rev. **D 83**, 073006 (2011), 1101.2755.
 - [7] J. Kopp, M. Maltoni, and T. Schwetz (2011), 1103.4570.
 - [8] J. Hamann, S. Hannestad, G. G. Raffelt, I. Tamborra, and Y. Y. Wong, Phys. Rev. Lett. **105**, 181301 (2010), 1006.5276.
 - [9] Y. Izotov and T. Thuan, Astrophys. J. **710**, L67 (2010), 1001.4440.
 - [10] E. Aver, K. A. Olive, and E. D. Skillman, JCAP **1005**, 003 (2010), 1001.5218.
 - [11] S. M. Bilenky, S. Pascoli, and S. Petcov, Phys. Rev. **D 64**, 113003 (2001), hep-ph/0104218.
 - [12] S. Goswami and W. Rodejohann, Phys. Rev. **D 73**, 113003 (2006), hep-ph/0512234.
 - [13] S. Goswami and W. Rodejohann, JHEP **0710**, 073 (2007), 0706.1462.
 - [14] A. S. Riis and S. Hannestad, JCAP **1102**, 011 (2011), 1008.1495.
 - [15] J. A. Barrett and J. Formaggio (2011), 1105.1326.
 - [16] H. Nunokawa, O. L. G. Peres, and R. Zukanovich Funchal, Phys. Lett. **B 562**, 279 (2003), hep-ph/0302039.
 - [17] S. Choubey, JHEP **12**, 014 (2007), 0709.1937.
 - [18] S. Razzaque and A. Smirnov (2011), 1104.1390.
 - [19] S. Choubey, N. Harries, and G. Ross, Phys. Rev. **D 76**, 073013 (2007), hep-ph/0703092.
 - [20] A. Palazzo, Phys. Rev. **D 83**, 113013 (2011), 1105.1705.
 - [21] J. R. Kristiansen and O. Elgaroy (2011), 1104.0704.
 - [22] P. Minkowski, Phys. Lett. **B 67**, 421 (1977).
 - [23] T. Yanagida, in *Proc. Workshop on the Baryon Number of the Universe and Unified Theories*, edited by O. Sawada and A. Sugamoto (1979), p. 95.
 - [24] M. Gell-Mann, P. Ramond, and R. Slansky, in *Supergravity*, edited by P. van Nieuwenhuizen and D. Freedman (1979), p. 315.
 - [25] R. N. Mohapatra and G. Senjanovic, Phys. Rev. Lett. **44**, 912 (1980).
 - [26] G. Altarelli and F. Feruglio, Rev. Mod. Phys. **82**, 2701 (2010), 1002.0211.
 - [27] H. Ishimori, T. Kobayashi, H. Ohki, Y. Shimizu, H. Okada, et al., Prog. Theor. Phys. Suppl. **183**, 1 (2010), 1003.3552.
 - [28] A. Y. Smirnov and R. Zukanovich Funchal, Phys. Rev. **D 74**, 013001 (2006), hep-ph/0603009.
 - [29] K. Abe et al. (T2K Collaboration) (2011), 1106.2822.
 - [30] L. Whitehead, *Recent results from MINOS*, http://www-numi.fnal.gov/pr_plots/.
 - [31] G. Fogli, E. Lisi, A. Marrone, A. Palazzo, and A. Rotunno, Phys. Rev. Lett. **101**, 141801 (2008), 0806.2649.
 - [32] M. Maltoni and T. Schwetz, PoS **IDM2008**, 072 (2008), 0812.3161.
 - [33] T. Schwetz, M. Tortola, and J. Valle, New J. Phys. **13**, 063004 (2011), 1103.0734.
 - [34] G. L. Fogli, E. Lisi, A. Marrone, A. Palazzo, and A. M. Rotunno (2011), 1106.6028.

- [35] D. Gibin, A. Guglielmi, F. Pietropaolo, C. Rubbia, and P. Sala (2011), 1106.4417.
- [36] W. Rodejohann (2011), 1106.1334.
- [37] S. Hannestad, Prog. Part. Nucl. Phys. **65**, 185 (2010), 1007.0658.
- [38] J. Hamann, J. Lesgourgues, and G. Mangano, JCAP **0803**, 004 (2008), 0712.2826.
- [39] G. Altarelli and F. Feruglio, Nucl. Phys. **B 720**, 64 (2005), hep-ph/0504165.
- [40] M. Honda and M. Tanimoto, Prog. Theor. Phys. **119**, 583 (2008), 0801.0181.
- [41] J. Barry and W. Rodejohann, Phys. Rev. **D 81**, 093002 (2010), 1003.2385.
- [42] A. de Gouvea, J. Jenkins, and N. Vasudevan, Phys. Rev. **D 75**, 013003 (2007), hep-ph/0608147.
- [43] T. Asaka, S. Blanchet, and M. Shaposhnikov, Phys. Lett. **B 631**, 151 (2005), hep-ph/0503065.
- [44] M. Shaposhnikov, Nucl.Phys. **B 763**, 49 (2007), hep-ph/0605047.
- [45] M. Lindner, A. Merle, and V. Niro, JCAP **1101**, 034 (2011), 1011.4950.
- [46] S. Petcov, Phys. Lett. **B 110**, 245 (1982).
- [47] S. Petcov and W. Rodejohann, Phys. Rev. **D 71**, 073002 (2005), hep-ph/0409135.
- [48] E. Chun, A. S. Joshipura, and A. Smirnov, Phys. Lett. **B 357**, 608 (1995), hep-ph/9505275.
- [49] Z.-Z. Xing, Chin. Phys. **C 32**, 96 (2008), 0706.0052.
- [50] J. D. Vergados, Y. Giomataris, and Y. N. Novikov (2011), 1105.3654.